Rheol Acta (2010) 49:119–129
DOI 10.1007/s00397-009-0415-3

ORIGINAL CONTRIBUTION

Extensional rheology of a shear-thickening cornstarch and water suspension

Erica E. Bischoff White · Manoj Chellamuthu · Jonathan P. Rothstein

Received: 16 July 2009 / Accepted: 30 November 2009 / Published online: 18 December 2009

Abstract A filament-stretching rheometer is used to measure the extensional viscosity of a shear-thickening suspension of cornstarch in water. The experiments are performed at a concentration of 55 wt.%. The shear rheology of these suspensions demonstrates a strong shear-thickening behavior. The extensional rheology of the suspensions demonstrates a Newtonian response at low extension rates. At moderate strain rates, the fluid strain hardens. The speed of the strain hardening and the extensional viscosity achieved increase quickly with increasing extension rate. Above a critical extension rate, the extensional viscosity goes through a maximum and the fluid filaments fail through a brittle fracture at a constant tensile stress. The glassy response of the suspension is likely the result of jamming of particles or clusters of particles at these high extension rates. This same mechanism is responsible for the shear thickening of these suspensions. In capillary breakup extensional rheometry, measurement of these suspensions demonstrates a divergence in the extensional viscosity as the fluid stops draining after a modest strain is accumulated.

Keywords Suspension · Thixotropy · Extensional flow · Elongational flow · Shear thickening

E. E. Bischoff White · M. Chellamuthu · J. P. Rothstein (✉)
Department of Mechanical and Industrial Engineering, University of Massachusetts, Amherst, MA 01003, USA
e-mail: rothstein@ecs.umass.edu

Introduction

The rheology and flow of colloidal suspensions has been a topic of great interest since Einstein's seminal work (Einstein 1906, 1911). Einstein showed that, in the dilute limit, the addition of spherical particles to a Newtonian solvent results in a first-order correction to the fluid viscosity $\eta = \eta_s (1 + 2.5\phi)$ where ϕ is the particle concentration and η_s is the viscosity of the suspending fluid (Einstein 1906, 1911; Happel and Brenner 1965). As the concentration is increased beyond the dilute limit, particle–particle interactions can produce long-range order which can result in non-Newtonian effects such as shear thinning or shear thickening of the fluid viscosity, the generation of nonzero normal stresses, and even the appearance of a yield stress at concentrations near maximum packing (Jeffreys and Acrivos 1976; Larson 1999). In this paper, we will focus on concentrated dilatant dispersions for which shear thickening has been observed.

The early investigations of shear-thickening systems were motivated by the need to mitigate the damage that the shear-thickening transition can have on processing equipment, to understand the flow of slurries, and to improve coating quality (Bender and Wagner 1996). Shear-thickening fluids are currently being utilized in a number of commercial applications including use in machine mounts, damping devices, and limited slip differentials (Helber et al. 1990; Laun et al. 1991). Additionally, it has recently been demonstrated that shear-thickening fluids, when incorporated into Kevlar vests and subjected to high-velocity projectiles, can dramatically improve both the performance and flexibility of the body armor (Lee et al. 2003).

The physical mechanism of shear thickening has been generally well understood for some time. Perhaps the best known example of shear thickening in the literature is the pioneering work of Hoffman (1972) who studied 1-μm diameter polyvinyl chloride (PVC) particles over a range of concentrations. Above a volume fraction of approximately $\phi > 1.5$, the suspensions demonstrated a discontinuity in their shear viscosity at a critical shear rate that decreased with increasing concentration. Hoffman (1972) was the first to couple shear-thickening rheological measurements with microstructural information obtained through light diffraction measurements. Below the critical shear rate, he observed diffraction patterns consistent with a two-dimensional hexagonal lattice of spheres. Hoffman (1972, 1974) interpreted this as particles forming and moving past each other in highly ordered layers; a theory that was first postulated by Reiner (1949). These fluids are often called dilatant because in order for the layers of particles to slide past each other they must first expand in the gradient direction (Pryce-Jones 1941). Thus, confinement can have a big effect on the response of these fluids in shear (Fall et al. 2008). Above the critical shear rate, Hoffman (1972, 1974) observed a diffuse diffraction pattern, suggesting that, at high shear rates, the particles move in a disordered way.

Over the last 30 years, a number of research groups have used a combination of numerical simulations and careful experiments to study the validity of the order-to-disorder transition first proposed by Hoffman as the source of shear thickening in concentrated suspensions. Recent experimental studies (Bender and Wagner 1996; Catherall et al. 2000; Fagan and Zukoski 1997; Laun et al. 1992; Maranzano and Wagner 2001) have shown that shear thickening can occur without a shear-induced order-to-disorder transition. Through measurements of rheology, turbidity, and small-angle neutron scattering under flow, Bender and Wagner (1996) showed that shear thickening occurs when attractive hydrodynamic shear forces overcome the Brownian repulsive forces in hard-sphere suspensions. They concluded that shear thickening results from a transition from a shear-induced ordered structure to the state of hydrodynamic clustering. Their measurements were consistent with the measurements of Barnes (1989) and the Stokesian dynamics simulations of Bossis and Brady (1984, 1989) which demonstrated that suspensions shear thicken at high Peclét numbers due to the formation of large clusters. At high concentrations, the shear-thickening transition can be discontinuous, which is likely the result of aggregates of clusters forming a jammed network (Cates et al. 1998; Farr et al. 1997).

Unlike the shear rheology of shear-thickening suspensions, which have been studied quite extensively, the extensional rheology of concentrated suspensions has been studied with significantly less scrutiny. The first reference to the behavior of concentrated suspensions in extensional flows dates back to Pryce-Jones (1941) who observed that dilatancy was an essential property for insuring spinnability in suspensions, although no quantitative data were presented. Despite this early observation, it was not until the 1970s that extensional viscosity measurements of suspensions were made (Kizior and Seyer 1974; Mewis and Metzner 1974; Takserman-Krozer and Ziabicki 1963). These experiments focused on dilute shear-thinning suspensions of rigid rods of different aspect ratios with Trouton ratios of greater than $Tr = \eta_E/\eta > 250$ achieved for the highest aspect ratio and concentration of fibers. Here, η and η_E are the shear and extensional viscosity of the suspension, respectively. The experimental extensional viscosity measurements were in good agreement with theoretical predictions of Batchelor (1971). A number of more recent studies have looked at the extensional viscosity of fiber suspensions in both Newtonian (Ma et al. 2008; Xu et al. 2005) and viscoelastic solvents (Férec et al. 2009; Metzner 1985).

More recently, Chellamuthu et al. (2009) investigated the extensional rheology of a shear-thickening fumed silica nanoparticle suspension using a filament-stretching rheometer. Below a critical extension rate, their measurements showed little strain hardening. At a critical extension rate, however, Chellamuthu et al. (2009) observed a dramatic increase in the rate and extent of strain hardening of the extensional viscosity similar to the thickening transition observed in shear. Light scattering measurements showed that the extensional hardening was due to the alignment of nanoparticles and the formation of long strings of aggregates in the flow. The fumed silica particles used in their study had a fractal chain-like structure (Raghavan and Khan 1997). One question this current study hopes to answer is whether extensional hardening can also be achieved in symmetric or nearly symmetric particles that exhibit shear thickening.

In this paper, the shear and extensional rheology of a suspension of 55 wt.% cornstarch and water are explored. Shear rheology measurements were performed to study the shear-thickening behavior of the suspension. A filament-stretching rheometer was then employed to study the effect of extension rate on the extensional viscosity of the suspension. Finally, capil-

lary breakup extensional rheology measurements were used to examine the dynamics of the flow leading up to the brittle filament failure observed during filament stretching.

Experimental methods

Sample preparation

A suspension of cornstarch (Argo) in water was prepared at a concentration of 55 wt.%. This corresponds to a volume fraction of $\phi = 35.5\%$ assuming a density of 1,550 kg/m^3 (Yang et al. 2005). As seen in Fig. 1, the cornstarch particles are polydisperse in size ranging from 5 to 15 μm in diameter with a facetted shape that is approximately spherical. This weight fraction was chosen to insure shear-thickening behavior while maintaining a workable solution. A number of much lower concentration samples were mixed; however, their extensional viscosity was too small to be measured by our filament-stretching rheometer. The samples were initially mixed by hand and then for a period of 15 min using a sonicator (Branson 2510) in order to obtain a uniform distribution of cornstarch particles within the suspension and to insure the particles where not aggregated.

Filament-stretching extensional rheometry

A filament-stretching extensional rheometer (FiSER), capable of imposing a homogeneous uniaxial extension on a fluid filament placed between its two endplates, was used to make simultaneous measurements of the evolution in the force and the midpoint radius. A complete description of the design and operating space of the filament-stretching rheometer used in these experiments can be found in Rothstein (2003) and Rothstein and McKinley (2002a, b) and a more detailed history of the technique can be found in the papers by the McKinley and Sridhar groups (Anna et al. 2001; McKinley and Sridhar 2002; Tirtaatmadja and Sridhar 1993).

The goal of extensional rheometry is to produce a motion of the two endplates such that the resulting extension rate imposed on the fluid filament:

$$\dot{\varepsilon} = -\frac{2}{R_{\mathrm{mid}}(t)}\frac{\mathrm{d}R_{\mathrm{mid}}(t)}{\mathrm{d}t} \tag{1}$$

is constant. The deformation imposed upon the fluid filament can be described in terms of a Hencky strain $\varepsilon = -2\ln(R_{\mathrm{mid}}/R_0)$ where R_0 is the initial midpoint radius of the fluid filament. The elastic tensile stress difference generated within the filament can be calculated from the algebraic sum of the total force measured by the load cell, F_z, if the weight of the fluid and the surface tension are taken into account while ignoring inertial effects (Szabo 1997):

$$\langle \tau_{zz} - \tau_{rr} \rangle = \frac{F_z}{\pi R_{\mathrm{mid}}^2} + \frac{1}{2}\frac{\rho g\left(\pi L_0 R_0^2\right)}{\pi R_{\mathrm{mid}}^2} - \frac{\sigma}{R_{\mathrm{mid}}} \tag{2}$$

where L_0 is the initial endplate separation, σ is the equilibrium surface tension of the fluid, and ρ is the density of the fluid. The extensional viscosity may be extracted from the principle elastic tensile stress and is often nondimensionalized as a Trouton ratio:

$$\eta_{\mathrm{E}}^{+} = \langle \tau_{zz} - \tau_{rr} \rangle / \dot{\varepsilon} \tag{3}$$

where η_{E}^{+} is the transient extensional viscosity and η_0 is the zero shear rate viscosity of the fluid.

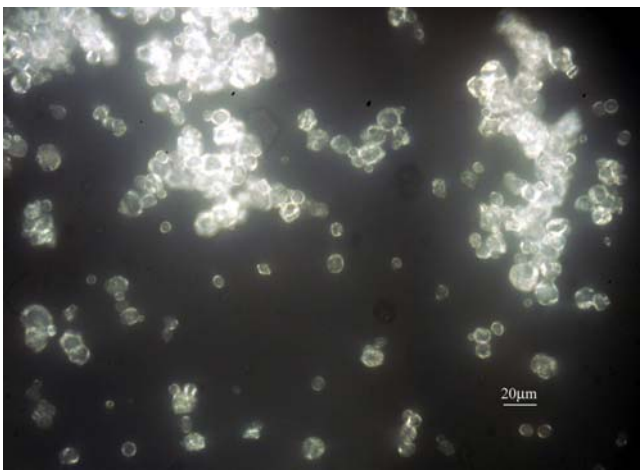

Fig. 1 Micrograph of cornstarch particles

Capillary breakup extensional rheometry

Capillary breakup extensional rheometry (CaBER) measurements have become an increasingly common technique for determining the extensional rheology of the less-concentrated and less-viscous fluids (Anna and McKinley 2001; Bazilevsky et al. 1990; Clasen et al. 2006; Entov and Hinch 1997; Kojic et al. 2006; McKinley and Tripathi 2000; Plog et al. 2005; Rodd et al. 2005; Stelter et al. 2000; Yesilata et al. 2006). The CaBER measurements presented here were performed using the filament-stretching rheometer described in the previous section. In all of the CaBER experiments presented here, an initial nearly cylindrical fluid sample is placed between two cylindrical plates and stretched

with an exponential profile, $L = L_0 \exp(\dot{\varepsilon}_0 t)$, at a constant extension rate $\dot{\varepsilon}_0 = 0.2\,\mathrm{s}^{-1}$ from an initial length of $L_0 = 2.5$ mm to a final length of $L_f = 5$ mm. The stretch is then stopped and the capillary thinning of the liquid bridge formed between the two endplates produces a uniaxial extensional flow that can be used to measure an apparent extensional viscosity of the test fluid. For these experiments, the stretch rates were chosen such that they were much greater than the inverse time scale for capillary drainage of the liquid bridge, $\dot{\varepsilon} >> \sigma/\eta_0 R_0$, but slow enough that extensional thickening would not occur during the initial step-stretch.

The breakup of the fluid filament is driven by capillary stresses and resisted by the extensional stresses developed within the flow. The extensional viscosity of a complex liquid solution can be determined by measuring the change in the filament diameter as a function of time. Papageorgiou (1995) showed that, for a Newtonian fluid of extensional viscosity η_E, the radius of the fluid filament will decay linearly with time, $R_{mid}(t) \propto (t_b - t)/\eta_E$, to the final breakup at t_b. Conversely, Entov and Hinch (1997) showed that, for a viscoelastic Oldroyd-B fluid with an extensional relaxation time λ_E, the radius will decay exponentially with time, $R_{mid}(t) \propto \exp(-t/3\lambda_E)$.

For a Newtonian fluid, the extension rate given by Eq. 1 will increase linearly with time, while for an ideal viscoelastic fluid, the extension rate is constant. For a number of less-ideal fluids, the extension rate achieved in the fluid filament can vary quite significantly with time (Miller et al. 2009; Tripathi et al. 2000). The evolution of an *apparent* extensional viscosity with this extension rate profile can be calculated by applying a force balance between capillary stresses and the viscous and elastic tensile stresses within the fluid filament (Anna and McKinley 2001):

$$\eta_E = \frac{\sigma/R_{mid}(t)}{\dot{\varepsilon}(t)} = \frac{-\sigma}{\mathrm{d}D_{mid}/\mathrm{d}t}. \quad (4)$$

To calculate the apparent extensional viscosity, the diameter measurements are carefully fit with a spline and then differentiated numerically (Miller 2007).

Results and discussion

High-concentration suspensions of cornstarch and water are well known to shear thicken in both steady and oscillatory shear flows (Fall et al. 2008; Merkt et al. 2004). Owing to their low cost and the ease of acquisition, this property of cornstarch and water solutions has made it a favorite in classrooms for demonstrating non-Newtonian fluid behavior. In Fig. 2, the steady shear rate viscosity is presented as a function of shear rate for our 55 wt.% suspension of cornstarch in water. The shear rheology of the suspensions was characterized using a stress-controlled rheometer (TA instruments, AR2000) with 40-mm parallel-plate geometry and a 1-mm gap. At low shear rates, the viscosity initially decreased with increasing shear rate. At a critical shear rate of approximately $\dot{\gamma}_{crit} \cong 8\,\mathrm{s}^{-1}$, the viscosity increased quickly with increasing shear rate. The magnitude of shear thickening saturated at a maximum shear viscosity of approximately $\eta \cong 20$ Pa·s; however, it is unclear if the flow is still viscometric at this point or if this plateau is due to slip or failure of the fluid within the parallel-plate rheometer.

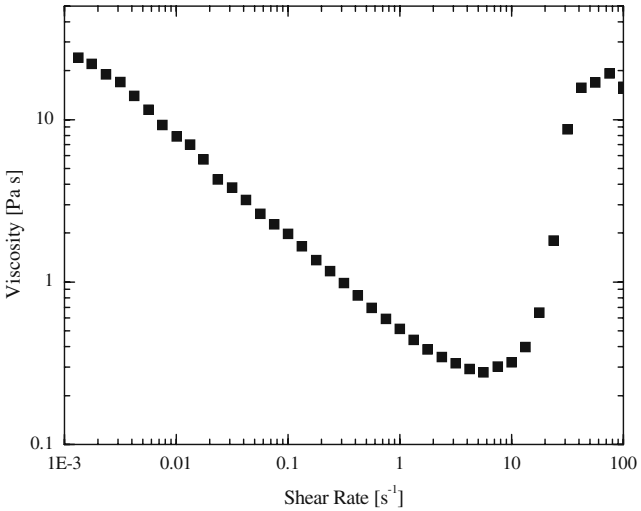

Fig. 2 Steady-shear rheology of 55 wt.% cornstarch in water suspension

The filament-stretching rheometer was used to conduct a series of stretches over a wide range of extension rates. All experiments were performed with an initial aspect ratio of $\Lambda = L_0/R_0 = 1.0$. Although this is the standard for filament-stretching measurements, the choice of aspect ratio can have a profound effect on one's ability to achieve a homogenous extensional flow everywhere within the fluid filament (Yao and Spiegelberg 2000). In filament stretching, a shear flow occurs near the two endplates during the early stages of the experiment. The strength of this flow and its influence on the resulting extensional viscosity measurements has been shown to decrease with increasing aspect ratio (McKinley and Sridhar 2002; Spiegelberg and McKinley 1996). Using a lubrication analysis valid in the limit of small aspect ratios, Spiegelberg and McKinley (1996) showed that the shear rate in the flow between the two plates is proportional to $\dot{\gamma} \propto \dot{\varepsilon}/\Lambda^2$.

Ideally, an aspect ratio much greater than one is desirable to eliminate any effects of shear from the extensional measurements; however, due to gravitational sagging, aspect ratios greater than one are not experimentally obtainable (Anna et al. 2001). This is especially important for shear-thickening fluids like the cornstarch and water solutions used here where, if the initial shear rate is too large, the suspension can transition from a fluid to a glassy system as the particles or clusters of particles jam during the start of the stretch before a homogeneous extensional flow can be achieved.

To work around this experimental limitation, a test protocol was incorporated which consisted of two distinct stretching phases (Sridhar et al. 2000). The first stretch phase was performed at an extension rate of $\dot{\varepsilon} = 0.20\,\mathrm{s}^{-1}$ to a final Hencky strain of $\varepsilon = 0.5$ in order to form a preliminary fluid filament of a higher aspect ratio. Upon completion of the first phase, a second much faster stretch rate between $0.3\,s^{-1} < \dot{\varepsilon} < 7\,s^{-1}$ was immediately imposed and continued until the filament failed. This experimental protocol is akin to a preshear step often imposed prior to shear rheology measurements. The initial stretch was performed at an extension rate well below the onset of extensional thickening where the fluid exhibits a Newtonian response and allowed a fluid filament to develop with limited shearing and little effect on the response of the fluid during the second phase of the stretch. After the initial stretch, the second phase of the stretch was essentially imposed on a filament with an aspect ratio of $\Lambda = 2.6$, thus reducing the shear rate near the endplates by a factor of nearly seven. A series of different initial stretch rates and strains were studied in order to optimize the test protocol. Changes to the initial strain rate below $\dot{\varepsilon} \leq 0.20\,\mathrm{s}^{-1}$ for a given initial strain were found to have no appreciable effect on the extensional rheology measured during the second phase of stretch. However, there is a lower limit to the initial strain rate below which the filament fails under capillary drainage before the higher extension rate can be imposed. The final strain of the initial stretch was chosen to be as large as possible without encountering capillary drainage effects. This protocol was used for all of the FiSER experiments presented in this paper so that all the filaments experienced the same initial flow history. All of the extensional viscosity and strain measurements are reported for the second phase of the stretch only.

In Fig. 3a, a representative plot of diameter decay as a function of time is presented for a series of extension rates varying from $\dot{\varepsilon} = 0.30\,\mathrm{s}^{-1}$ to $\dot{\varepsilon} = 2.0\,\mathrm{s}^{-1}$. The linear decay of the diameter with time on the semilog

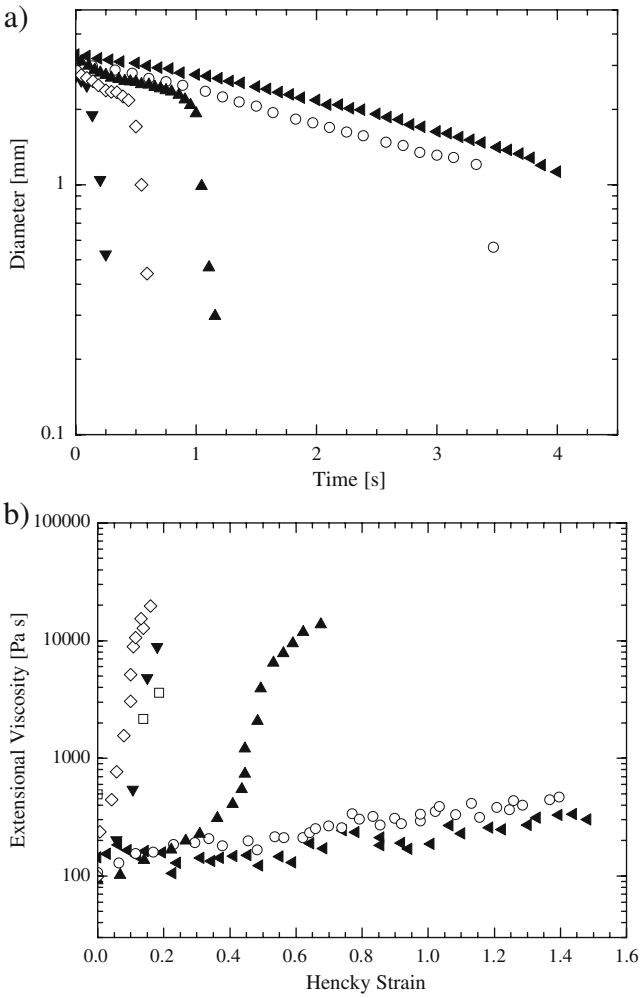

Fig. 3 Transient extensional rheology measurements of 55 wt.% cornstarch in water including **a** the diameter decay as a function of time and **b** the extensional viscosity as a function of accumulated Hencky strain. The data include stretches performed at extension rates of ◀ $\dot{\varepsilon} = 0.3\,\mathrm{s}^{-1}$, ○ $\dot{\varepsilon} = 0.5\,\mathrm{s}^{-1}$, ▲ $\dot{\varepsilon} = 0.6\,\mathrm{s}^{-1}$, ◇ $\dot{\varepsilon} = 0.9\,\mathrm{s}^{-1}$, ▼ $\dot{\varepsilon} = 2.0\,\mathrm{s}^{-1}$, and □ $\dot{\varepsilon} = 4.0\,\mathrm{s}^{-1}$

plot in Fig. 3a demonstrates that, by using the iterative method of Orr and Sridhar (1999), a constant extension rate is achieved. Unfortunately, this method cannot maintain a constant extension rate during filament failure which can be quite dramatic for these cornstarch and water solutions. The filament failure can be seen in Fig. 3a where the diameter data deviates from a linear decay at the end of the higher extension rate experiments. Just prior to the onset of filament failure, the extensional viscosity tends to go through a maximum. To avoid the difficulty of interpreting the extensional rheology data after the onset of filament failure where the extension rate is no longer constant, the extensional viscosity data in Fig. 3b are only reported up to the point of the maximum extensional viscosity. Bach et al.

(2003) and Rasmussen et al. (2005) have shown that, if one uses a closed-loop feedback control algorithm rather than the iterative Orr–Sridhar method, that data can be collected at a constant extension rate even beyond the maximum in the extensional viscosity as the filament begins to fail. An attempt was made to implement a similar scheme in our filament-stretching rheometer; however, the dynamics for these low viscosity systems were too fast for us to control satisfactorily. Such a control scheme appears to be more applicable to higher-viscosity fluids like polymer melts.

In Fig. 3b, a representative plot of the extensional viscosity as a function of accumulated Hencky strain is presented for a series of extension rates varying from $\dot{\varepsilon} = 0.30\,\mathrm{s}^{-1}$ to $\dot{\varepsilon} = 4.0\,\mathrm{s}^{-1}$. Below an extension rate of $\dot{\varepsilon} < 0.30\,\mathrm{s}^{-1}$, the force exerted on the endplates was below the resolution of the 10-g force transducer. As seen in all of Fig. 3b, no strain hardening is observed at low strain rates. Although a clear zero shear rate viscosity was not observed in the shear rheology, based on an approximate zero shear rate viscosity of $\eta_0 \approx 30$ Pa s, a Newtonian response of $Tr = 3$ should result in an extensional viscosity of $\eta_E \approx 100$ Pa s. This is consistent with the low extension rate measurements presented in Fig. 3b. In this regime, a steady-state value of the extensional rheology is achieved which is essentially insensitive to changes in extension rate. As shown in the high-speed image in Fig. 4a, the fluid filament drains and eventually fails through capillary-driven pinch off after significant deformation.

Above an extension rate of $\dot{\varepsilon} > 0.30\,\mathrm{s}^{-1}$, but below an extension rate of $\dot{\varepsilon} < 1.0\,\mathrm{s}^{-1}$, the fluid begins to strain harden and the extensional viscosity begins to increase with increasing extension rate. As was seen previously for suspensions of shear-thickening fumed silica particles (Chellamuthu et al. 2009), the speed and magnitude of the strain hardening increases remarkably quickly with extension rate. Because the extensional viscosity did not always reach steady state before the end of the stretch, the maximum value of the extensional viscosity is presented in Fig. 5 as a function of extension rate. The extensional viscosity for the cornstarch in water suspensions shows a sharp extensional thickening transition which is very similar in magnitude and form to the shear-thickening transition observed in steady shear flows. As seen in Fig. 4b, this region is characterized by the formation of long elastic fluid filaments similar to those observed in filament-stretching measurements of polymeric fluids and worm-like micelle solutions (Chen and Rothstein 2004; McKinley and Sridhar 2002). At these extension rates, the filament tends to fail through a pinch off near the bottom endplate after a modest strain had been accumulated. At these transitional extension rates, the total accumulated Hencky strain and the extensional viscosity

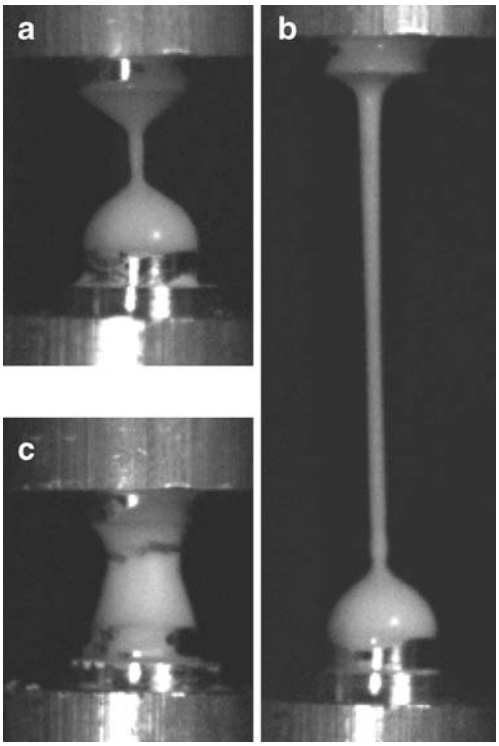

Fig. 4 High-speed images of 55 wt.% cornstarch in water suspension being stretched. The images demonstrate **a** the Newtonian response of the fluid filament at a low extension rate of $\dot{\varepsilon} = 0.3\,\mathrm{s}^{-1}$, **b** the strain-hardening response at a moderate extension rate of $\dot{\varepsilon} = 0.9\,\mathrm{s}^{-1}$, and **c** the solid-like brittle fracture of the fluid filament at a large extension rate of $\dot{\varepsilon} = 1.5\,\mathrm{s}^{-1}$

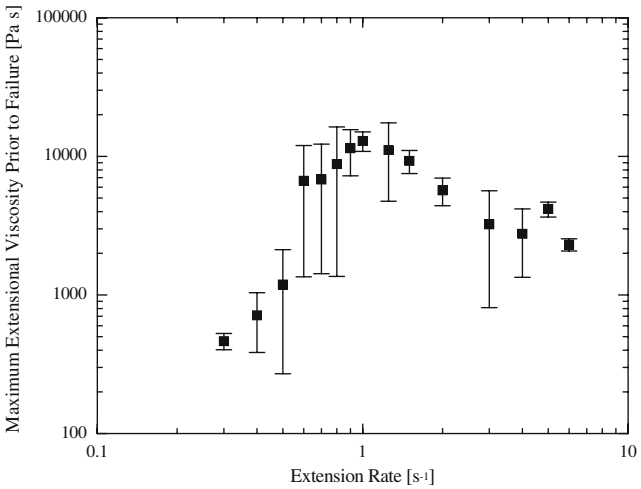

Fig. 5 Maximum extensional viscosity achieved before filament failure for a 55 wt.% cornstarch in water suspension

measured at filament failure fluctuate significantly. This accounts for the large error bars on the steady-state extensional viscosity measurements shown in Fig. 5 and the tensile stress measurements presented in Fig. 6. The data points in Figs. 5 and 6 represent an average value taken from as many as seven and as few as four independent experiments on fresh samples. The error bars represent the certainty of the data to 95% confidence.

Above a critical extension rate of $\dot{\varepsilon} > 1.0\,\mathrm{s}^{-1}$, the maximum extensional viscosity goes through a maximum and begins to decrease with increasing extension rate. Within this region, the fluid exhibits a glassy behavior. As seen in Fig. 4c, the fluid fails through a brittle fracture reminiscent of solid failure under extensional loadings well before a steady-state extensional viscosity can be reached. Similar filament failures have been observed for heavily cross-linked rubbers and even linear polymer deformed under very high extension rates (Joshi and Denn 2004; Malkin and Petrie 1997; Renardy 2004; Vinogradov et al. 1975). As was observed by a number of researchers in the past (Malkin and Petrie 1997), at very high extension rates, the fluid filaments experience very little strain before rupture. However, unlike the work of Vinogradov et al. (1975) who worked with polystyrene and PVC, the ultimate strength (or stress at failure) of the cornstarch and water suspensions does not decrease with increasing extension rate. Instead, Fig. 6 shows that the ultimate strength levels off above $\dot{\varepsilon} > 1.0\,\mathrm{s}^{-1}$ and the brittle failure of the fluid filament appears to occur at a critical tensile stress difference of approximately $(\tau_{zz} - \tau_{rr})_c \cong 15,000\,\mathrm{Pa}$. The constant ultimate strength is consistent with the measurements of Smith (1958) who studied GR-S rubbers. This constant value of tensile stress at filament failure accounts for the steady decrease of the extensional viscosity with increasing extension rate observed in Fig. 5. Given a constant tensile stress, Eq. 3 dictates that the extensional viscosity in the glassy region should decrease as $\eta_E \propto \dot{\varepsilon}^{-1}$ in this glass-like zone. These observations suggests that the physical mechanism for the sharp extensional thickening transition is the same as it is in shear; namely, particle or clusters of particles forming a jammed interconnected network.

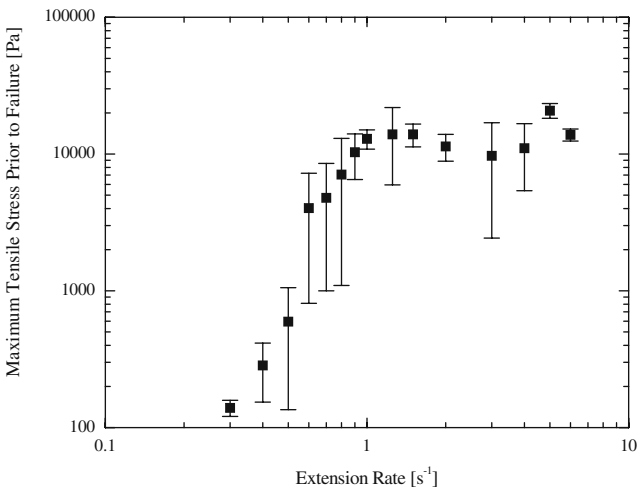

Fig. 6 Maximum tensile stress measured before filament failure in extensional flow for a 55 wt.% cornstarch in water suspension

These extensional rheology results are similar to the recent measurements of shear-thickening fumed silica nanoparticle suspensions (Chellamuthu et al. 2009). However, unlike the cornstarch in water suspensions, the nanoparticle suspensions did not exhibit a glassy response at high extension rates. The nanoparticle suspensions achieved a steady-state extensional viscosity for all extension rates tested and failed not through a brittle fracture, but through ductile elastocapillary failure of the fluid filament. These observations, coupled with the light scattering measurements of Chellamuthu et al. (2009), suggest that the extensional thickening for the nanoparticle suspensions was not due to particle or cluster jamming, but rather due to the formation of long string-like clusters of nanoparticles aligned in the flow direction.

It is interesting to note that, although the mechanism for shear and extensional thickening appear to be the same, the extensional thickening occurs at rates that are at least one order of magnitude less than in shear. Thus, extensional flow appears to be more effective at jamming these suspensions than shear flow. This observation may be surprising at first because a strong extensional flow might be expected to break down weakly aggregated structures. However, the relative rheological enhancement in extensional flows compared to shear flows might be attributable to the lack of rotation in extensional flow which could be responsible for slowing the formation or even breaking down clusters of particles in shear flows. Another possibility is that the compressive flow in the radial direction may locally increase the packing of the cornstarch particles before they are stretched axially, making it easier for the particles to jam.

To investigate the jamming transition further, a series of measurements were made using CaBER. The advantage of this technique, as opposed to FiSER, is that the extensional flow is self-driven and not imposed. Thus, the fluid is not expected to fail through a brittle fracture, but should drain completely thus giving us access to the response of the fluid at much larger Hencky strains. However, as one can observe in the diameter

decay of the cornstarch in water suspension presented in Fig. 7, the expected result was not achieved. The initial decay of the diameter is inversely proportional to time and thus follows a Newtonian response as described by Papageorgiou (1995). However, after about one half of a second, a knee is observed in the diameter data. At this point, the evolution of the diameter with time slows down to the point that the filament appears to have frozen. Thus, even under capillary-driven drainage, these cornstarch and water systems jam. If this were a FiSER experiment, the filament would fail at this point; however, for the CaBER experiment, the filament simply stops evolving. A close inspection of the data reveals that the filament is not completely frozen, but is still evolving with time, albeit very slowly with time. There are examples in the literature where similar CaBER responses were observed. Tripathi et al. (2000) showed that, for polymer solutions where the solvent was extremely volatile, that evaporation could cause the fluid to solidify before the filament had completely drained. In our case, the evaporation rate of water over the course of the CaBER experiment is very small and the observations are more likely the result of the jamming of cornstarch particles or clusters of particles in the suspension.

A spline was fit to the diameter data and then differentiated with time in order to calculate the evolution of the strain, strain rate, and extensional viscosity from Eq. 4. The extensional viscosity is plotted against accumulated strain in Fig. 8a and against extension rate in Fig. 8b. At small strains, the extensional viscosity is found to be approximately $\eta_E \approx 100$ Pa s which is again approximately the expected Newtonian response of $Tr = 3$. As the strain approaches $\varepsilon = 0.425$, the extensional viscosity diverges, reaching a maximum value of approximately $\eta_{max} \approx 16{,}000$ Pa s. It is important to note that the exact value of this maximum is sensitive to the precise form of the spline used to fit the diameter decay. This maximum agrees quite well with the maximum value of the extensional viscosity measured through FiSER. If we evaluate the extensional viscosity as a function of strain rate, we find that the transition from Newtonian response to jamming occurs at around an extension rate of $\dot{\varepsilon} > 1.4\,s^{-1}$ which also agrees quite well with the FiSER results.

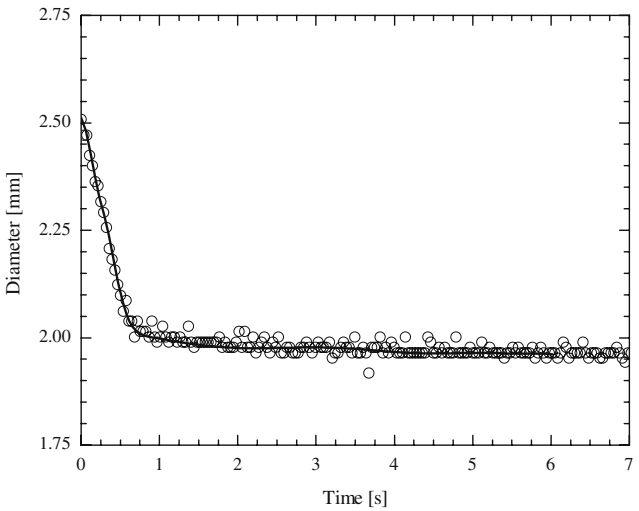

Fig. 7 Diameter decay measurements for a CaBER measurement of a 55 wt.% cornstarch in water suspension. The spline used to fit the data and calculate the extensional viscosity, *thick line*, is superimposed on top of the experimental data, ○

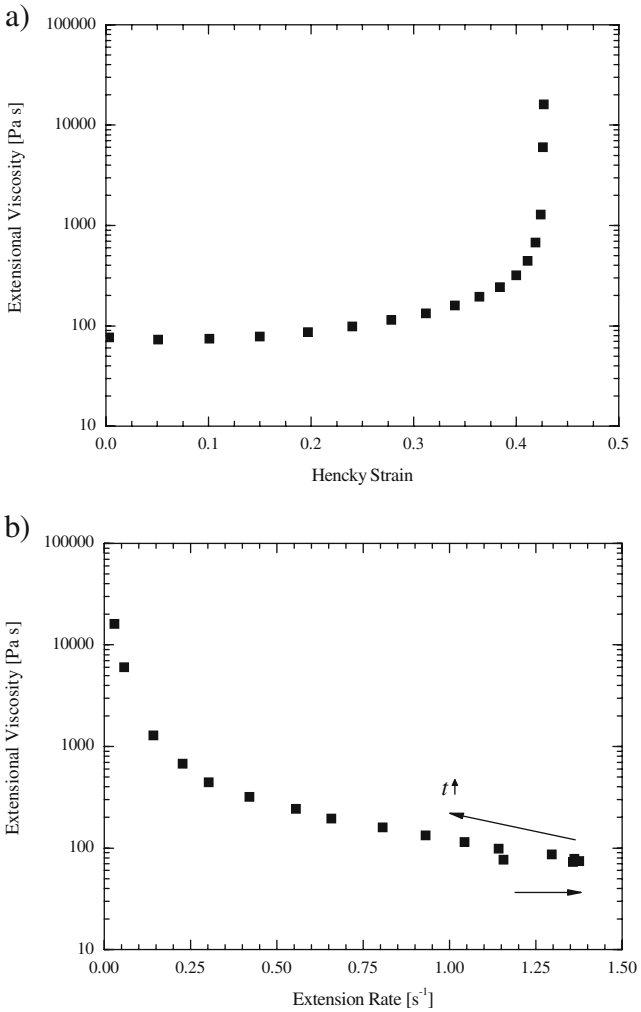

Fig. 8 Extensional viscosity measurements as a function of **a** Hencky strain and **b** resulting strain rate for the CaBER measurement of a 55 wt.% cornstarch in water suspension

Conclusion

The extensional properties of a shear-thickening cornstarch in water suspension were studied using both filament stretching and capillary breakup rheometry. The shear rheology of a series of the 55 wt.% cornstarch in water suspension demonstrated a shear-thinning behavior at low strain rates and shear-thickening transition at high shear rates. The shear thickening in these systems is likely due to the formation of large clusters of particles that form interconnected jammed network under high shear rates. These observations are consistent with previous work involving similar systems in the literature.

A series of extensional rheology measurements were performed using a filament-stretching rheometer. At low extension rates, the fluid exhibited a Newtonian response with an extensional viscosity equal to three times the zero shear rate viscosity. At moderate extension rates, the fluid demonstrated modest strain hardening and the formation of long coherent fluid filaments. However, at a critical extension rate, a dramatic increase in both the rate and magnitude of the strain hardening was observed with increasing extensional rate. This observed extensional thickening of the steady-state or maximum extensional viscosity was similar in form to the shear-thickening response. At these high extension rates, the fluid filament did not fail through an elastocapillary necking, but rather through a brittle failure. This glassy fracture was found to occur at a constant value of extensional stress, independent of the imposed extension rate. These observations would suggest that, like in shear, the dramatic increase in strain hardening is most likely due to the aggregation of particles or clusters of particles to form an interconnected jammed network across the fluid filament with a finite ultimate strength.

These observations were further reinforced by CaBER measurements. Under capillary breakup, the resulting extensional flow is self-driven and not imposed, making it possible to observe the extensional viscosity in the absence of the brittle filament failures observed using FiSER. The diameter of the fluid filament was initially observed to decay quite quickly. However, at a modest strain, an abrupt deceleration of the diameter decay was observed, leading to the eventual cessation of the flow and a divergence of the extensional viscosity. These observations again reinforce the argument that the extensional thickening and brittle failure of the fluid filament is the result of jamming of the cornstarch particles under strong extensional flows.

Acknowledgements The authors would like to thank the National Science Foundation for the generous support of this research under grant CBET-0547150 and through the MRSEC and the CHM at the University of Massachusetts, Amherst.

References

Anna SL, McKinley GH (2001) Elasto-capillary thinning and breakup of model elastic liquids. J Rheol 45:115–138

Anna SL, McKinley GH, Nguyen DA, Sridhar T, Muller SJ, Huang J, James DF (2001) An inter-laboratory comparison of measurements from filament stretching rheometers using common test fluids. J Rheol 45:83–114

Bach A, Almdal K, Rasmussen HK, Hassager O (2003) Elongational viscosity of narrow molar mass distribution polystyrene. Macromolecules 36:5174–5179

Barnes HA (1989) Shear-thickening in suspensions of nonaggregrating solid particles dispersed in Newtonian liquids. J Rheol 33:329–366

Batchelor GK (1971) The stress generated in a non-dilute suspension of elongated particles by pure straining motion. J Fluid Mech 46:813–829

Bazilevsky AV, Entov VM, Rozhkov AN (1990) Liquid filament microrheometer and some of its applications. Proceedings of the Third European Rheology Conference, Edinburgh

Bender J, Wagner NJ (1996) Reversible shear thickening in monodisperse and bidisperse colloidal dispersions. J Rheol 40:899–916

Bossis G, Brady JF (1984) Dynamic simulation of sheared suspensions. 1. General method. J Chem Phys 80:5141–5154

Bossis G, Brady JF (1989) The rheology of Brownian suspensions. J Chem Phys 91:1866–1874

Cates ME, Wittmer JP, Bouchaud JP, Claudin P (1998) Jamming, force chains, and fragile matter. Phys Rev Lett 81:1841–1844

Catherall AA, Melrose JR, Ball RC (2000) Shear thickening and order-disorder effects in concentrated colloids at high shear rates. J Rheol 44:1–25

Chellamuthu M, Arndt EM, Rothstein JP (2009) Extensional rheology of shear-thickening nanoparticle suspensions. Soft Matter 5:2117–2124

Chen S, Rothstein JP (2004) Flow of a wormlike micelle solution past a falling sphere. J Non-Newton Fluid Mech 116:205–234

Clasen C, Plog JP, Kulicke WM, Owens M, Macosko C, Scriven LE, Verani M, McKinley GH (2006) How dilute are dilute solutions in extensional flows? J Rheol 50:849–881

Einstein A (1906) Eine neue Bestimmung der Moleküldimensionen. Ann Phys 19:289–306

Einstein A (1911) Berichtigung zu meiner Arbeit: Eine neue Bestimmung der Moleküldimensionen. Ann Phys 34: 591–592

Entov VM, Hinch EJ (1997) Effect of a spectrum of relaxation times on the capillary thinning of a filament of elastic liquid. J Non-Newton Fluid Mech 72:31–53

Fagan ME, Zukoski CF (1997) The rheology of charge stabilized silica suspensions. J Rheol 41:373–397

Fall A, Huang N, Bertrand F, Ovarlez G, Bonn D (2008) Shear thickening of cornstarch suspensions as a reentrant jamming transition. Phys Rev Lett 100:018301

Farr RS, Melrose JR, Ball RC (1997) Kinetic theory of jamming in hard-sphere startup flows. Phys Rev E 55:7203–7211

Férec J, Heuzey M-C, Pérez-González J, Vargas Ld, Ausias G, Carreau PJ (2009) Investigation of the rheological properties

of short glass fiber-filled polypropylene in extensional flow. Rheol Acta 48:59–72
Happel J, Brenner H (1965) Low Reynolds number hydrodynamics. Prentice-Hall, Englewood Cliffs
Helber R, Doncker F, Bung R (1990) Vibration attenuation by passive stiffness switching mounts. J Sound Vib 138:47–57
Hoffman RL (1972) Discontinuous and dilatant viscosity behavior in concentrated suspensions. I. Observation of a flow instability. J Rheol 16:155–173
Hoffman RL (1974) Discontinuous and dilatant viscosity behavior in concentrated suspensions. II. Theory and experimental tests. J Colloid Interface Sci 46:491–506
Jeffreys DJ, Acrivos A (1976) The rheological properties of suspensions of rigid particles. AIChE J 22:417–432
Joshi YM, Denn MM (2004) Failure and recovery of entangled polymer melts in elongational flow. In: Binding DM, Walters K (eds) Rheology reviews. British Society of Rheology, Aberystwyth
Kizior TE, Seyer FA (1974) Axial stress in elongational flow of fiber suspension. J Rheol 18:271–285
Kojic N, Bico J, Clasen C, McKinley GH (2006) Ex vivo rheology of spider silk. J Exp Biol 209:4355–4362
Larson RG (1999) The structure and rheology of complex fluids. Oxford University Press, New York
Laun HM, Bung R, Hess S, Loose W, Hess O, Hahn K, Hadicke E, Hingmann R, Schmidt F, Lindner P (1992) Rheological and small-angle neutron-scattering investigation of shear-induced particle structures of concentrated polymer dispersions submitted to plane Poiseuille and Couette-flow. J Rheol 36:743–787
Laun HM, Bung R, Schmidt F (1991) Rheology of extremely shear thickening polymer dispersions (passively viscosity switching fluids). J Rheol 35:999–1034
Lee YS, Wetzel ED, Wagner NJ (2003) The ballistic impact characteristics of Kevlar woven fabrics impregnated with a colloidal shear thickening fluid. J Mater Sci 38:2825–2833
Ma AWK, Chinesta F, Tuladhar T, Mackley MR (2008) Filament stretching of carbon nanotube suspensions. Rheol Acta 47:447–457
Malkin AY, Petrie CJS (1997) Some conditions for rupture of polymer liquids in extension. J Rheol 41:1–25
Maranzano BJ, Wagner NJ (2001) The effects of interparticle interactions and particle size on reversible shear thickening: hard-sphere colloidal dispersions. J Rheol 45:1205–1222
McKinley GH, Sridhar T (2002) Filament stretching rheometry. Annu Rev Fluid Mech 34:375–415
McKinley GH, Tripathi A (2000) How to extract the Newtonian viscosity from capilary breakup measurements in a filament rheometer. J Rheol 44:653–670
Merkt FS, Deegan RD, Goldman DI, Rericha EC, Swinney HL (2004) Persistent holes in a fluid. Phys Rev Lett 92:184501
Metzner AB (1985) Rheology of suspensions in polymeric liquids. J Rheol 29:739–775
Mewis J, Metzner AB (1974) The rheological properties of suspensions of fibres in Newtonian fluids subjected to extensional deformations. J Fluid Mech 62:593–600
Miller E (2007) The dynamics and rheology of shear-banding wormlike micelles and other non-Newtonian fluids. Thesis, University of Massachusetts
Miller E, Clasen C, Rothstein JP (2009) The effect of step-stretch parameters on capillary breakup extensional rheology (CaBER) measurements. Rheol Acta 48:625–639
Orr NV, Sridhar T (1999) Probing the dynamics of polymer solutions in extensional flow using step strain rate experiments. J Non-Newton Fluid Mech 82:203–232
Papageorgiou DT (1995) On the breakup of viscous liquid threads. Phys Fluids 7:1529–1544
Plog JP, Kulicke WM, Clasen C (2005) Influence of the molar mass distribution on the elongational behaviour of polymer solutions in capillary breakup. Appl Rheol 15: 28–37
Pryce-Jones J (1941) Experiments on thixotropic and other anomalous fluids with a new rotation viscometer. J Sci Instrum 18:39–48
Raghavan SR, Khan SA (1997) Shear-thickening response of fumed silica suspensions under steady and oscillatory shear. J Colloid Interface Sci 185:57–67
Rasmussen HK, Nielsen JK, Bach A, Hassager O (2005) Viscosity overshoot in the start-up of uniaxial elongation of LDPE melts. J Rheol 49:369–381
Reiner M (1949) Deformation and flow. Lewis, London
Renardy M (2004) Self-similar breakup of non-Newtonian fluid jets. In: Binding DM, Walters K (eds) Rheology reviews. The British Society of Rheology, Aberystwyth
Rodd LE, Scott TP, Cooper-White JJ, McKinley GH (2005) Capillary break-up rheometry of low-viscosity elastic fluids. Appl Rheol 15:12–27
Rothstein JP (2003) Transient extensional rheology of wormlike micelle solutions. J Rheol 47:1227–1247
Rothstein JP, McKinley GH (2002a) A comparison of the stress and birefringence growth of dilute, semi-dilute and concentrated polymer solutions in uniaxial extensional flows. J Non-Newton Fluid Mech 108:275–290
Rothstein JP, McKinley GH (2002b) Inhomogeneous transient uniaxial extensional rheometry. J Rheol 46:1419–1443
Smith TL (1958) Dependence of the ultimate properties of a GR-S rubber on strain rate and temperature. J Polym Sci 32: 99–113
Spiegelberg SH, McKinley GH (1996) Stress relaxation and elastic decohesion of viscoelastic polymer solutions in extensional flow. J Non-Newton Fluid Mech 67:49–76
Sridhar T, Nguyen DA, Fuller GG (2000) Birefringence and stress growth in uniaxial extension of polymer solutions. J Non-Newton Fluid Mech 90:299–315
Stelter M, Brenn G, Yarin AL, Singh RP, Durst F (2000) Validation and application of a novel elongational device for polymer solutions. J Rheol 44:595–616
Szabo P (1997) Transient filament stretching rheometry I: force balance analysis. Rheol Acta 36:277–284
Takserman-Krozer R, Ziabicki A (1963) Behavior of polymer solutions in a velocity field with parallel gradient. I. Orientation of rigid ellipsoids in a dilute solution. J Polym Sci Part A 1:491–506
Tirtaatmadja V, Sridhar T (1993) A filament stretching device for measurement of extensional viscosity. J Rheol 37:1133–1160
Tripathi A, Whitingstall P, McKinley GH (2000) Using filament stretching rheometry to predict stand formations and processability in adhesives and other non-Newtonian fluids. Rheol Acta 39:321–337
Vinogradov GV, Malkin AY, Volosevitch VV, Shatalov VP, Yudin VP (1975) Flow, high-elastic (recoverable) deformations and rupture of uncured high molecular weight linear polymers in uniaxial extension. J Polym Sci Polym Phys Ed 13:1721–1735

Xu J, Chatterjee S, Koelling KW, Wang Y, Bechtel SE (2005) Shear and extensional rheology of carbon nanofiber suspensions. Rheol Acta 44:537–562

Yang J, Sliva A, Banerjee A, Dave RN, Pfeffe R (2005) Dry particle coating for improving the flowability of cohesive powders. Powder Technol 158:21–33

Yao M, Spiegelberg SH (2000) Dynamics of weakly strain hardening fluids in filament stretching devices. J Non-Newton Fluid Mech 89:1–43

Yesilata B, Clasen C, McKinley GH (2006) Nonlinear shear and extensional flow dynamics of wormlike surfactant solutions. J Non-Newton Fluid Mech 133:73–90